

# The Hydrodynamic Performance Examination of a New Floating Breakwater Configuration

Yasser El Saie<sup>1</sup>, Ayman El Sayed<sup>2</sup>, Haitham Ehab<sup>3</sup>, Ahmed Balah<sup>4</sup>

<sup>1</sup> Associate professor, Head of Civil Department, The Higher Institute of Engineering, El Shorouk Academy, Egypt.

<sup>2</sup> Professor of Harbor Engineering and Marine Structures, Irrigation and Hydraulics Department, Faculty of Engineering, Ain Shams University, Egypt.

<sup>3</sup> Instructor in civil engineering department, The Higher Institute of Engineering, El Shorouk Academy, Egypt  
Currently Pursuing M.SC Program in Civil Engineering, Irrigation and Hydraulics Department, Faculty of Engineering, Ain Shams University, Egypt.

<sup>4</sup> Lecturer, Irrigation and Hydraulics Department, Faculty of Engineering, Ain shams University, Egypt.

Received: 01 Dec 2022; Received in revised form: 30 Dec 2022; Accepted: 06 Jan 2023; Available online: 14 Jan 2023

**Abstract**— It is critical to protect coastal and offshore structures. Most current studies and scientific investigations are centered on how to protect seashore with an efficient and cost-effective system. This study involved the testing of a new floating breakwater configuration (FB). A series of experiments were carried out in the lab of The Higher Institute of Engineering (El-shorouk City) on the new model and the traditional vertical plane FB without a curved face to compare their behaviours and performance in wave attenuation. The incident, reflected, and transmitted wave heights were measured, and the coefficients of reflection, transmission, and energy dissipation were calculated using these measurements. In terms of hydrodynamic performance, the curved-face floating breakwater outperformed the traditional vertical floating breakwater, according to the study's highlights. The curved face model significantly reduced wave transmission values when compared to the traditional vertical configuration. The greater the concavity of the curve, the better the model handles waves, especially when the wave steepness is low.

**Keywords**— Curved face floating breakwater, Reflection Coefficient, Transmission coefficient, Energy dissipation coefficient, shore protection.

## I. INTRODUCTION

The parts of land that face the seas, oceans, marines, and ports are known as coastlines. Breakwaters are wave attenuators, which are used to dissipate wave energy and protect coastlines from wave attacks. Breakwaters are divided into two types: conventional and non-conventional. The growth of offshore and maritime activities increases the demand for larger ports, making conventional bottom breakwater construction difficult. Floating breakwaters have been widely used in the protection of seashores, coastlines, ports, and marines over the last few decades. Indeed, 90% of wave energy is distributed along a depth three times the wave height below the water's surface.

Various researchers and scientists worked on this issue from (Fang He et al., 2012) to (S Rahman et al., 2022). [1] Fang He et al. (2012) installed pneumatic chambers with the original rectangular floating breakwater; the increased mass and inertia of the model has a significant effect on wave attenuation. Furthermore, the energy is dissipated more effectively in the front chambers than in the back chambers. [2] Chun-Yan Ji et al. (2016) investigated the hydrodynamic performance of a new floating breakwater configuration. The effect of beam and oblique waves on a ten-cylinder floating breakwater with ten mesh cages and eighteen connectors was investigated. Overall, the results demonstrated the impact of this configuration on energy dissipation and wave attenuation. [3] Chun-Yan et al. (2017) studied the effect of wave attacks on a new structure, A Cylindrical Dual Pontoon-Net floating

breakwater (CDPNFB) attached to one or more rows of plane net experimental model. This study discovered that increasing net porosity lowers the reflection coefficient and vice versa for the transmission coefficient. Furthermore, the more cylinders used, the greater the wave blocking achieved by the model. [4] Chun-Yan Ji et al. (2019) investigated the hydrodynamic performance of a double-row rectangular floating breakwater with porous plates through a series of experiments. The experiments were carried out in a wave flume measuring 40m\*0.8m\*1.4m. Overall, the results showed that porous plates with small motion responses and mooring forces have a significant effect on wave attenuation.

[5] Chun-Yan Ji et al. (2015) compared a new type of floating breakwater with double pontoons and a box type, and found that the new configuration, a cylindrical floating breakwater with a flexible mesh cage, outperformed the other two types in long and high waves. [6] Chun-Yan Ji et al. (2016) conducted an experimental study of four types of floating breakwaters; the results showed that the mesh cage model was more effective than the other types. [7] Zhiwen Yang et al. (2018) investigated the effectiveness of a new floating breakwater against wave attacks. This structure is made up of a water ballast double floating box with a vertical plate. The findings of this study revealed that water ballast attenuates the incident wave more than dry ballast, and that the height of the vertical plate is effective in reducing wave transmission. [8] Chun-Yan Ji et al. (2019) conducted a series of experiments to compare single and double-row floating breakwaters. In terms of wave attenuation, the double-row performed better than the single-row. [9] S Rahman et al. (2020) theoretically and experimentally compared a modified pontoon type with a pi-type breakwater. The study's findings revealed that the developed pontoon type model has less transmission coefficient than pi-type model also the peak value of the heave motion is smaller than that of the pi-type.

The curved face floating breakwater model was tested against regular wave attacks in this study to determine the effectiveness of the studied parameters on its efficiency. The goal of this paper is to try a new configuration based on previous studies. Experiments were performed on the models under the influence of various wave conditions in order to test the model's functionality before comparing the results.

## II. EXPERIMENTAL WORK

This part shows the experimental equipment and model used in the experiments. Also, it states the steps that were taken to carry out the experimental work.

This article can be downloaded from here: [www.ijaems.com](http://www.ijaems.com)

### 2.1 Experimental Equipment

A series of experiments were conducted in two-dimensional wave flume in the Hydraulics Laboratory of the Higher Institute of engineering (El Shorouk City). The flume is 12 m long, 0.5 m width and 0.6 m deep. The wave maker used is fly wheel type connected by steel rod to paddle. Two wave absorbers from sloped graded gravel were used in the tests to prevent standing wave from reflection. The absorbers were installed in the flume with suitable slopes ranges from (2:1 to 5:1) and its size ranging from (0.5 – 3 cm) in diameter. The mooring lines used during the experiments were steel wires covered by a plastic layer. Figures 1 and 2 show the wave flume and schematic diagram for the flume.



Fig. 1: The Wave Flume

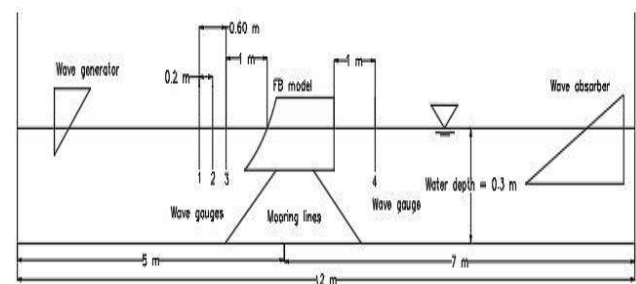


Fig. 2: Schematic Diagram of The Model in The Flume

An ultrasonic instrument (Wave Staff XB) used to determine the wave motion showing the wave heights versus time interval on a schematic diagram. The wave staff XB was installed in three positions to indicate incident, reflection, and transmission wave heights. The instrument was mounted on a small steel frame moves on the sides of the flume. The spacing between wave gauges applied were based on ([10] Mansard, and Funke, 1980) suggestions to calculate the relative distances between wave gauges.  $X_{12} = L/10, L/6 \leq X_{13} \leq L/3$

Where  $L$  is the wavelength,  $X_{12}$  is the distance between the first two gauges positions and  $X_{13}$  is the distance between the first and third wave gauges in the line of wave propagation.

Each pattern was examined under the effect of five different wave heights, to complete this objective, about 135 runs were carried out and the wave heights were measured to determine the reflection, transmission, and energy dissipation coefficients, as the wavelength and wave heights are constant in all runs, then the incident wave heights were measured in the beginning of the experimental work. The wave gauges (1),(2) and (3) were used to determine the reflected wave height and wave gauge (4) was used to determine transmitted wave height.

**2.2 Experimental Model**

The supposed models were examined due to the proposed experimental program. The tested models were fixed to the base of the flume by steel wires with anchors fixed in the base. The parts of the model are two blocks (48 x 30 x 5 cm), one block (48 x 30 x 20 cm) and three curved parts with apex angles (30°, 60°, 90°).

The experimental model used in this study is made of fiber and out covered by a timber layer, the pattern used in experimental work was to investigate the effect of each of the following parameters: The floating breakwater width (w), The floating breakwater draft (d) and the curvature of breakwater face (θ). The studied parameters and the model parts are shown in figure 3 and figure 4 respectively.

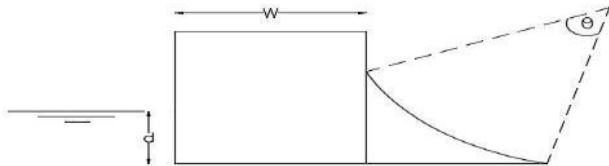


Fig. 3: The Studied Parameters



Fig. 4: Experimental Model Parts and its installation

**2.3 Experimental Steps**

A series of experiments were carried out in a 2D wave flume to study the effectiveness of the curved face floating breakwater. The new configuration was studied by testing various widths (20, 25 and 30 cm), different draft values (2, 10 and 20 cm) and three apex angles (30, 60 and 90 degrees). Each model was examined against five different

wave heights (16, 11, 6.25, 4.5 and 2.5 cm) with constant wavelength approximately equals 248 cm and water depth equals 30 cm. The incident reflected and transmitted wave heights were calculated using the plot from the wave staff XB illustrated in figure 5. Also, the wave staff XB used in experiments is illustrated in figure 6. Both maximum and minimum heights were recognized from the wave staff plot, then the calculation of the wave heights was as follows:

$$\text{Incident wave height } (H_I) = \frac{H_{\max} + H_{\min}}{2} \quad (1)$$

$$\text{Reflected wave height } (H_R) = \frac{H_{\max} - H_{\min}}{2} \quad (2)$$

$$\text{Transmitted wave height } (H_T) = H_{\max} - H_{\min} \quad (3)$$

$$\text{Reflection Coefficient } (C_r) = \frac{H_R}{H_I} \quad (4)$$

$$\text{Transmission Coefficient } (C_t) = \frac{H_T}{H_I} \quad (5)$$

$$\text{Energy Dissipation Coefficient } (C_d) = \sqrt{1 - C_t^2 - C_r^2} \quad (6)$$

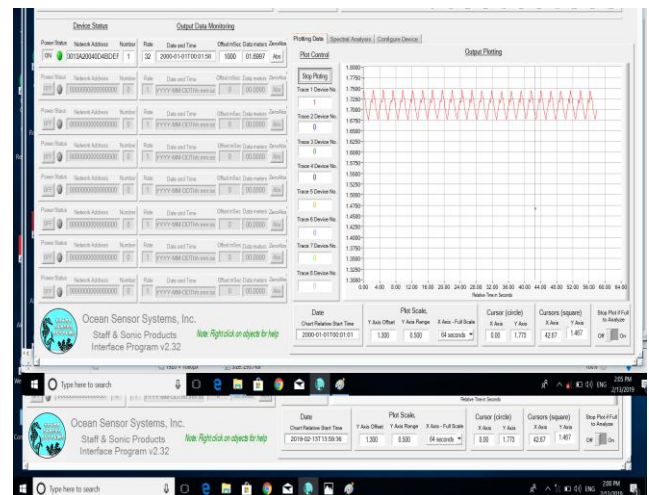


Fig. 5: The Wave Staff XB Plot



Fig. 6: The Wave Staff XB

## 2.4 Hydraulic Modeling

The water viscosity and surface tension are not the dominant factors that affect the phenomenon. While the gravity force and inertia are main parameters affecting the phenomenon. Thus, the Froude law is used in simulating the phenomenon.

$$F_N = \frac{v}{\sqrt{gL}} \quad (7)$$

$$F_N (\text{model}) = F_N (\text{prototype})$$

$$\left(\frac{v}{\sqrt{gL}}\right)_m = \left(\frac{v}{\sqrt{gL}}\right)_p \quad (8)$$

$$L_r = \frac{L_m}{L_p} \quad (9)$$

$$V_r = \frac{v_m}{v_p} = \frac{\sqrt{L_m}}{\sqrt{L_p}} = \sqrt{L_r} \quad (10)$$

$$T_r = \frac{T_m}{T_p} = \frac{\frac{L_m}{v_m}}{\frac{L_p}{v_p}} = \frac{L_r}{v_r} \quad (11)$$

$$T_r = \frac{L_r}{\sqrt{L_r}} = \sqrt{L_r} \quad (12)$$

Considering Wave Characteristics, Wave Celerity (C):

$$C = \frac{L}{T} \quad (13)$$

$$C_r = \frac{C_m}{C_p} = \frac{L_r}{T_r} \quad (14)$$

$$C_r = \frac{L_r}{\sqrt{L_r}} = T_r \quad (15)$$

Depending on the dimensions of the flume and the wave conditions (length, height) that will be applied on the models. A ratio of 1:20 was selected for the construction of the curved face floating breakwater model.

## III. EXPERIMENTAL RESULTS

The hydrodynamic performance of the curved face floating breakwater models was investigated by measuring wave reflection and transmission heights then calculating reflection, transmission and energy dissipation coefficients. Finally, a comparison was held between the tested apex angles of curved faces used in the experiments.

### 3.1 Effect of Apex angle on reflection coefficient

The applied experiments showed the role of the curvature of the facing curve to wave attacks. The 30-, 60- and 90-degree curves were tested with different widths, drafts and five wave heights. The results proved that as the apex angle decreases which leads to the increment of curvature the reflection coefficient increases. this was highlighted as

This article can be downloaded from here: [www.ijaems.com](http://www.ijaems.com)

the 30-degree curve with 30 cm width, 20 cm draft gives the maximum values of reflection coefficients, on the other hand, the 90-degree curve when fitted with the same width and draft gives less values of reflection coefficients as shown in figure 7.

Figure 7 shows that the 30-degree curve recorded better results than the 60 degree and 90-degree curves, as it resists the wave motion more than the other two curves. These words could be more discussed with statistics that showed that the 30-degree curve reflected the incident wave with range from 88% to 97% for the five values of wave steepness. Thus, the 90-degree curve gave results from 84% to 92%. The 60-degree curve recorded values in between the 30 degree and 90-degree curve. The reflection coefficients produced from the tests of vertical face floating breakwater range from 82% to 90%. These results shows that the effectiveness of 30-degree curve in wave attenuation when compared with other curves and vertical face. also, it shows that the increment of the reflection coefficient with decreasing value of wave steepness attacking the curved face floating breakwater model. In addition to that, the curved face behavior is more efficient in low values of wave steepness than high values.

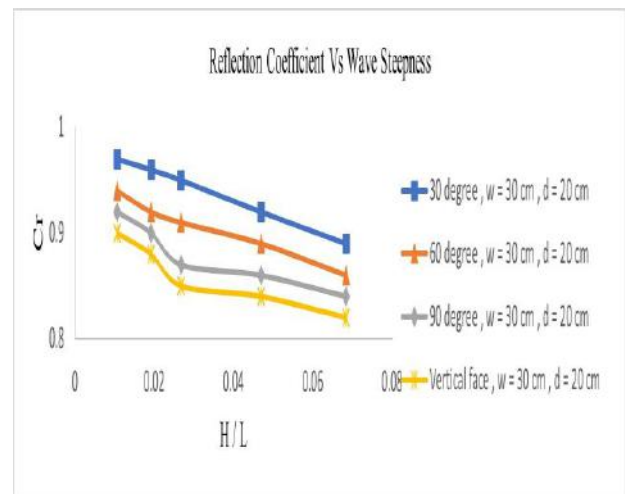


Fig. 7. Reflection Coefficient Vs Wave Steepness for Different Examined Curvatures & Width = 30 cm

### 3.2 Effect of Apex angle on transmission coefficient

The hydrodynamic performance of the floating breakwater is determined mainly by the transmission coefficient resulted from experiments carried out on the model. The highest values of transmission coefficients were resulted from the 90-degree curve, but less values were investigated from the tested 30-degree curve. The values of transmission coefficients recorded by the 30-degree curve illustrate the efficiency of this curvature in facing wave when comparing the experimental results of the three

tested curves, the 30-degree curve showed the best performance by decreasing the transmitting wave from the coming incident wave, while the other two curves gave more values of transmission coefficients than the 30-degree curve as shown in figure 8.

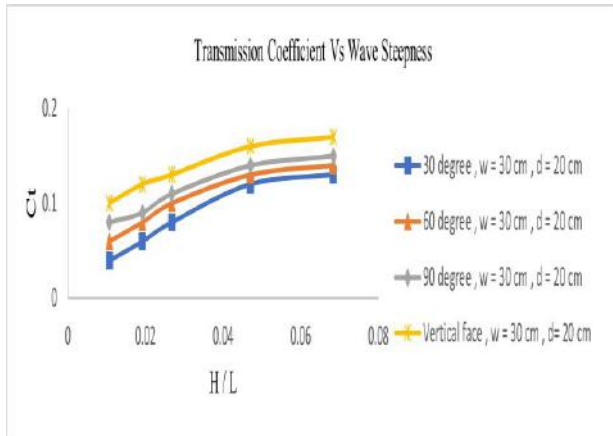


Fig. 8. Transmission Coefficient Vs Wave Steepness for Different Examined Curvatures & Width = 30 cm

### 3.3 Effect of Apex angle on Energy dissipation coefficient

The energy dissipation coefficient was calculated using the values of reflection and transmission coefficients. Figure 9 shows that by increasing the apex angle of curved surface, the energy dissipated from the incident wave increases. the vertical face floating breakwater recorded the highest energy dissipation coefficients values.

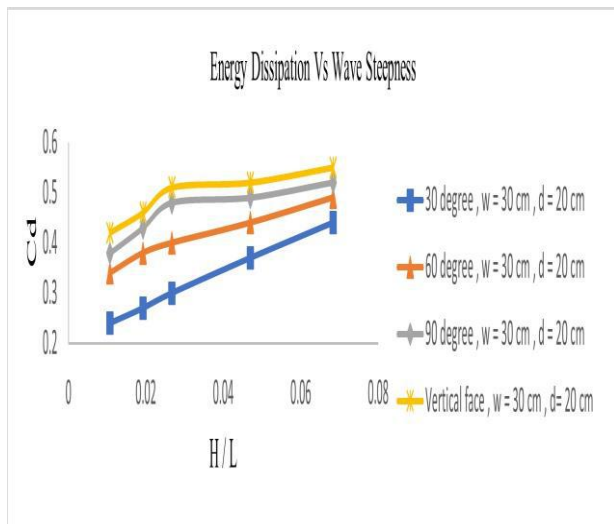


Fig. 9. Energy Dissipation Coefficient Vs Wave Steepness for Different Examined Curvatures & Width = 30 cm

### 3.4 Effect of width relative to wavelength on the hydrodynamic performance

The ratio of width relative to wavelength indicates the energy dissipated from the floating breakwater. the wavelength in the conducted experiments was 248 cm and the three widths used were 20, 25 and 30 cm. Figures 10, 11 and 12 showed the reflection, transmission and energy dissipation coefficients versus the width to wave length ratio (W/L). The coefficients shown in the figures are average values as for each width, the model was examined by five different wave heights and draft values. The increment of this ratio lowers the transmission coefficient for floating breakwaters and adjust the hydrodynamic performance against wave attacks.

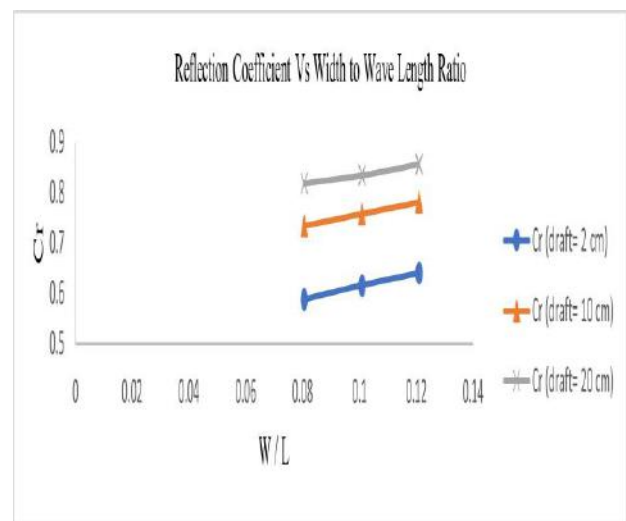


Fig. 10. Reflection Coefficient Vs Width to Wavelength ratio with different drafts

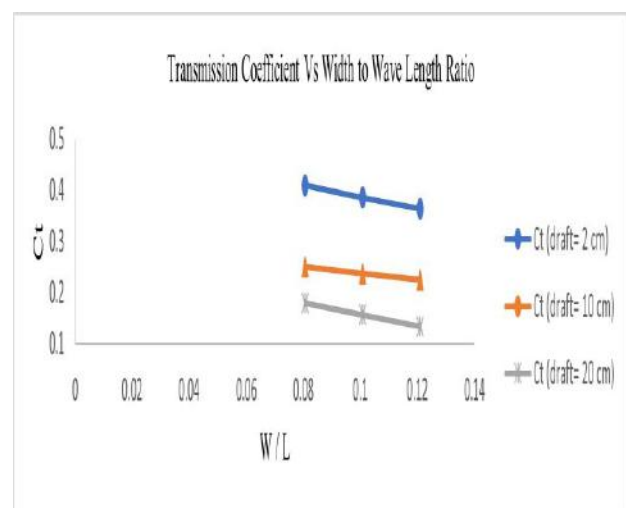


Fig. 11. Transmission Coefficient Vs Width to Wavelength ratio with different drafts

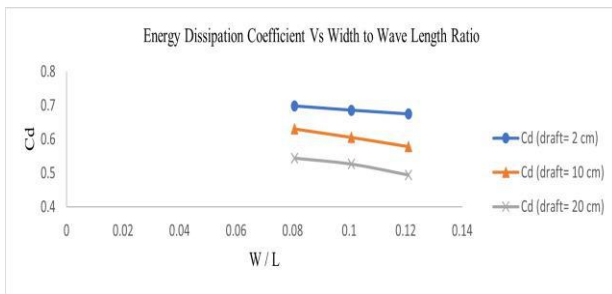


Fig. 12. Energy Dissipation Coefficient Vs Width to Wavelength ratio with different drafts

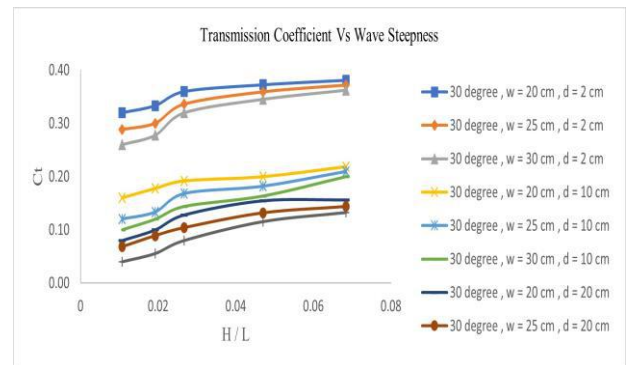


Fig. 14. Transmission Coefficient Vs Wave Steepness for 30-degree curvature with different widths and drafts

### 3.5 Effect of width and draft on curved face floating breakwater performance

The results showed that the best performance recorded for the examined model when the tested model was 30 cm width, 20 cm draft and 30-degree curvature, while the least hydrodynamic performance in wave attenuation and damping when the 20 cm width, 2 cm draft and 90 degree was used.

Figures 13 and 14 illustrated showed that the performance of the 30-degree curve increases with the increment of width and draft. The best performance was when the 30 cm width and 20 cm draft were used. On the other hand, the 20 cm width and 2 cm draft gave the weakest results in the tests.

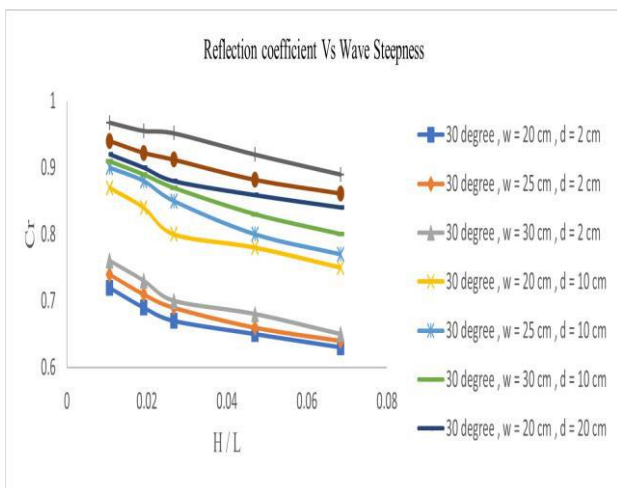


Fig. 13. Reflection Coefficient Vs Wave Steepness for 30-degree curvature with different widths and drafts

## IV. ANALYSIS AND DISCUSSIONS

The experimental results demonstrate the effect of increasing the width and draught of the floating breakwater on the development of its performance. In addition to the effect of curvature on wave reflection and transmission by studying three different curvatures as previously discussed. When the results of the three curved surfaces were compared, it was discovered that the 30-degree curvature performed better in wave attenuation than the others. As a result, the curvature of the surface facing the wave attacks has a significant impact on the performance of the floating breakwater. The coefficients of reflection, transmission, and energy dissipation were measured for a variety of configurations with varying wave heights. These coefficients, particularly transmission, indicate the resistance of waves to the floating breakwater. The results of the examined models were compared, and graphical charts were created to determine the best coefficients. Furthermore, studying the results of this paper and comparing them to the performance of other floating breakwaters will result in useful data and increased knowledge in the field of floating breakwaters. Table 1 summarizes the experimental findings.

## V. V. CONCLUSION

This study's findings concentrated on the effect of a curved face floating breakwater against regular wave attacks in a 2D wave flume. To investigate the hydrodynamic performance of a new configuration of floating breakwater model, experiments were carried out. According to the findings of this study, the greater the concavity of the curved face floating breakwater, the better the performance of the new type of floating breakwater when compared to the original vertical face floating breakwater. As is well known, the width and draft of floating breakwaters play an important role in increasing the reflection coefficient and decreasing the transmission coefficient. In this study, the

30 cm width and 20 cm draft produce the best results when compared to the other widths and drafts used. The reflection coefficient rises by around 25% and the transmission coefficient falls by 28% compared to the recorded values for 20 cm width and 2 cm draft, as shown in figures 7 and 8. The effectiveness of the curved face is directly proportional to the wave steepness decrement. The curved face floating breakwater is better than the vertical face floating breakwater in terms of hydrodynamic performance. Curved faces have a higher reflection coefficient than vertical faces. The average percentage increase in reflection coefficient as values change from low wave steepness to high wave steepness is around 7% for 30-degree curvature, 4% for 60-degree curvature, and 2% for 90-degree curvature. While the transmission coefficient decreases by 4.5%, 3%, and 2% for 30, 60, and

90-degree curvature, respectively as shown in table 1 for all other investigated configurations.

Based on previous research ([11] Koutandos et al., 2005; [12] Tolba et al., 1998) and various studies applied to floating breakwater (box type...).....etc., the studied new configuration is similar to the ordinary box type floating breakwater, i.e. it is a curved part attached to a box. As a result, the study's findings recommend designing and employing this new configuration when the water depth to wavelength ratio is 0.12, the floating breakwater depth to wave length ratio is 1, and the draught to water depth ratio is 0.67. These ratios are similar to those of the box type.

Table 1: Studied Parameters and Ranges of Coefficients

Studying Parameters			Ranges (%)		
Curvature	Width	Draft	$C_r$	$C_t$	$C_d$
30°	20 cm	2 cm	62.5 to 72	32 to 38.13	61.56 to 68.12
30°	25 cm	2 cm	64 to 74	28.8 to 37.19	60.78 to 67.18
30°	30 cm	2 cm	65 to 76	26 to 36.25	59.57 to 66.79
30°	20 cm	10 cm	75 to 90	16 to 21.88	40.55 to 62.42
30°	25 cm	10 cm	76.88 to 92	12 to 20.94	37.31 to 60.43
30°	30 cm	10 cm	77.81 to 96	6 to 20	27.35 to 59.54
30°	20 cm	20 cm	84.06 to 92	10 to 15.63	37.89 to 51.86
30°	25 cm	20 cm	86.13 to 94	6.8 to 14.38	33.43 to 48.74
30°	30 cm	20 cm	87.5 to 96.8	4 to 13.25	24.77 to 46.56
60°	20 cm	2 cm	58.75 to 66	33.2 to 39.38	22.71 to 24.99
60°	25 cm	2 cm	61.56 to 70	31.2 to 38.13	64.24 to 68.97
60°	30 cm	2 cm	63.75 to 74	28 to 37.19	61.16 to 67.48
60°	20 cm	10 cm	72.50 to 84	18 to 22.81	51.19 to 64.99
60°	25 cm	10 cm	74.38 to 88	15.2 to 21.88	45 to 63.17
60°	30 cm	10 cm	75.94 to 92	10 to 20.94	37.89 to 61.60
60°	20 cm	20 cm	82.5 to 88	12 to 16.56	45.96 to 54.03
60°	25 cm	20 cm	84.38 to 92	8.8 to 15.31	38.19 to 51.44
60°	30 cm	20 cm	85.94 to 94	6 to 14.06	33.59 to 49.16
90°	20 cm	2 cm	58.13 to 64	37.2 to 40.63	67.23 to 70.51

90°	25 cm	2 cm	59.06 to 68	34 to 39.38	64.96 to 70.44
90°	30 cm	2 cm	60.94 to 72	30 to 38.13	62.58 to 69.52
90°	20 cm	10 cm	70.63 to 80	22 to 23.75	55.82 to 66.70
90°	25 cm	10 cm	72.5 to 82	20 to 22.81	53.63 to 64.99
90°	30 cm	10 cm	74.38 to 88	18 to 21.88	43.95 to 63.17
90°	20 cm	20 cm	81.56 to 86.4	14 to 17.5	48.36 to 55.15
90°	25 cm	20 cm	82.5 to 88.8	11.2 to 15.94	44.60 to 54.22
90°	30 cm	20 cm	84.38 to 92	8 to 15	38.37 to 51.54
Vertical	20 cm	2 cm	55.94 to 62	39.2 to 42.81	67.97 to 70.98
Vertical	25 cm	2 cm	57.81 to 66	35.6 to 40.94	66.16 to 70.58
Vertical	30 cm	2 cm	58.75 to 69.2	32.8 to 39.69	64.31 to 70.52
Vertical	20 cm	10 cm	68.75 to 77.6	22.8 to 26.88	58.81 to 67.46
Vertical	25 cm	10 cm	70.88 to 79.6	22 to 24.88	56.39 to 66.01
Vertical	30 cm	10 cm	71.88 to 83.2	20.4 to 23.94	51.59 to 65.28
Vertical	20 cm	20 cm	79.69 to 84	16 to 20.13	51.85 to 56.96
Vertical	25 cm	20 cm	80.94 to 86	12.8 to 17.94	49.40 to 55.92
Vertical	30 cm	20 cm	81.88 to 90	9.2 to 16.88	42.61 to 54.88

### ACKNOWLEDGEMENTS

The authors are grateful for El- Shorouk Academy for funding and lab facilities.

### REFERENCES

- [1] Fang, H.; Zhenhua, H., and Adrian, W.K.L., 2012. Hydrodynamic performance of a rectangular floating breakwater with and without pneumatic chambers: An experimental study, *Ocean engineering*, 51, 16-27.
- [2] Chun-Yan, J.; Xiang, C.; Jie, C.; Oleg, G., and Atilla, I., 2016. Experimental study on configuration optimization of floating breakwaters, *Ocean engineering*, 117, 302-310.
- [3] Chun-Yan, J.; Yong, C.; Ke, Y., and Gaidai, O., 2017. Numerical and experimental investigation of hydrodynamic performance of a cylindrical dual pontoon-net floating breakwater, *Ocean engineering*, 129, 1-16.
- [4] Chun-Yan, J.; Xiang- Qian. B.; Yong, C., and Ke, Y., 2019. Experimental study of hydrodynamic performance for double-row rectangular floating breakwaters with porous plates, *Ships and Offshore structures*, 14:7, 737-746, DOI: [10.1080/17445302.2018.1558521](https://doi.org/10.1080/17445302.2018.1558521).
- [5] Chun-Yan, J.; Yong, C.; Jie, C.; Zhiming, Y., and Oleg. G., 2015. Hydrodynamic performance of floating breakwaters in long wave regime: An experimental study, *Ocean engineering*, 152, 154-166.
- [6] Chun-Yan, J.; Yu-Chan, G.; Jie, C.; Zhi-Ming, Y., and Xiao-Jian M., 2016. 3D experimental study on a cylindrical floating breakwater system, *Ocean engineering* 125, 38-50.
- [7] Zhiwen, Y.; Mingxiao, X.; Zhiliang, G.; Ting, X.; Weijun, G.; Xinran, J., and Chunguang, Y., 2018. Experimental investigation on hydrodynamic effectiveness of a water ballast type floating breakwater, *Ocean engineering*, 167, 77-94.
- [8] Rahman, S.; Baeda, A.Y.; Achmad, A., and Jamal, R.F., 2020. Performance of a new floating breakwater, *IOP Conf. Ser.: Mater. Sci. Eng.* **875** 012081.
- [9] Chun-Yan, J.; Ren-Shi, Z.; Jie, C., and Zhi-Lei, W., 2019. Experimental evaluation of wave transmission and dynamics of double-row floating breakwaters. *Ocean engineering*, 145(4):04019013.
- [10] Mansard, E.P.D. and Funke, E.R., 1980. The measurement of incident and reflected spectra using a least squares method, *Proceedings of the 17<sup>th</sup> International Conference on Coastal Engineering*, Sydney, Australia, 154-172.
- [11] Koutandos, E.; Prinos, P., and Gironella, X., 2005. Floating breakwaters under regular and irregular wave forcing: reflection and transmission characteristics, *Journal of Hydraulic Research* Vol. 43, No. 2, pp. 174–188 © 2005 International Association of Hydraulic Engineering and Research.
- [12] Tolba, E.R.A.S., 1998. "Behavior of Floating Breakwaters Under Wave Action". PhD. Thesis, Suez Canal University.